SIAM J. SCI. COMPUT.
Vol. 40, No. 6, pp. A3982–A4006

MULTIPLE SCALAR AUXILIARY VARIABLE (MSAV) APPROACH AND ITS APPLICATION TO THE PHASE-FIELD VESICLE MEMBRANE MODEL*

QING CHENG† AND JIE SHEN‡

Abstract. We consider in this paper gradient flows with disparate terms in the free energy that cannot be efficiently handled with the scalar auxiliary variable (SAV) approach, and we develop the multiple scalar auxiliary variable (MSAV) approach to deal with these cases. We apply the MSAV approach to the phase-field vesicle membrane (PF-VMEM) model which, in addition to some usual nonlinear terms in the free energy, has two additional penalty terms to enforce the volume and surface area. The MSAV approach enjoys the same computational advantages as the SAV approach but can handle free energies with multiple disparate terms such as the volume and surface area constraints in the PF-VMEM model. The MSAV schemes are unconditional energy stable and second-order accurate in time and lead to decoupled elliptic equations with constant coefficients to solve at each time step. Hence, these schemes are easy to implement and extremely efficient when coupled with an adaptive time stepping. Ample numerical results are presented to validate the stability and accuracy of the MSAV schemes.

Key words. phase-field, vesicle membrane, gradient flow, SAV approach, energy stability

AMS subject classifications. 65M12, 35K20, 35K35, 35K55, 65Z05

DOI. 10.1137/18M1166961

1. Introduction.

Recently, the so-called scalar auxiliary variable (SAV) approach is developed in [17, 18]. This approach is inspired by the invariant energy quadratization (IEQ) approach [21] but fixes most, if not all, of its shortcomings. While the SAV approach can be applied in principle to a large class of gradient flows, our numerical experiments indicate that it cannot produce correct numerical solutions for some gradient flows with disparate nonlinear terms such as those with penalty terms to enforce certain geometric constraints, unless exceedingly small time steps are used. The main reason is that these disparate nonlinear terms behave very differently and cannot be properly handled with a single SAV. This fact motivates us to develop the multiple scalar auxiliary variable (MSAV) approach in this paper to handle such situations. We consider, as a particular example, the phase-field vesicle membrane (PF-VMEM) model which, in addition to some usual nonlinear terms in the free energy, has two additional penalty terms to enforce the volume and surface area.

Biological vesicle membranes have been widely studied in biology, biophysics, and bioengineering. Accurate modeling and simulation of morphological evolution of vesicles present a great challenge due to the variety of equilibrium shapes assumed by vesicles in biological experiments. A pioneering work on single-phase lipid membrane

*Submitted to the journal's Methods and Algorithms for Scientific Computing section January 25, 2018; accepted for publication (in revised form) October 8, 2018; published electronically November 29, 2018.

http://www.siam.org/journals/sisc/40-6/M116696.html

Funding: This work was supported in part by NSF grants DMS-1620262, DMS-1720442, and AFOSR FA9550-16-1-0102 and NSFC grants 91630204, 11421110001, and 51661135011.

†School of Mathematical Sciences and Fujian Provincial Key Laboratory on Mathematical Modeling and High Performance Scientific Computing, Xiamen University, Xiamen, Fujian, People's Republic of China, 361005 (chengqing@stu.xmu.edu.cn).

‡Corresponding author. Department of Mathematics, Purdue University, West Lafayette, IN 47907 (shen7@purdue.edu).

was carried out by Canham, Evans, and Helfrich [1, 2, 12] in which the so-called sharp interface elastic bending energy is derived. On the other hand, by introducing a phase variable to describe the mean curvature of the membrane surface area, the authors of [4, 5, 6] have used the phase-field approach to approximate the elastic bending energy. The phase-field approach has since been used to study various kinds of vesicles, such as multicomponent vesicles [13, 19], vesicle-substrate adhesion [25], and vesicle-vesicle adhesion problems [10]. The main challenge in designing efficient and accurate numerical schemes for these models is to preserve the thermodynamically consistent dissipation law at the discrete level while imposing physical constraints such as conservation of volume and surface area.

A popular strategy to design energy stable time discretization schemes for gradient flows and phase-field models is the so-called convex splitting method [7, 8, 16, 24]. However, it appears to be difficult to apply it for the vesicle membrane model with volume and surface area constraints. Many other attempts have been made for this model, such as the stabilized semi-implicit method [3], exponential time discretization scheme [20], nonlinear scheme [11], and IEQ scheme [22]. All these numerical schemes are first-order accurate except the second-order scheme by the IEQ approach in [22]. However, the IEQ approach leads to a coupled linear system with complicated variable coefficients at each time step that is still expensive to solve. The SAV approach [18] leads to decoupled linear systems with constant coefficients so it is very efficient, but it failed to deliver correct numerical solutions with reasonable time steps. Therefore, we shall introduce multiple SAVs to deal with the volume and surface area constraints. More precisely, since the volume penalty term leads to a linear term in the PDE system so it can be treated implicitly along with other linear terms, we introduce one additional SAV for the surface area constraint to formulate an equivalent MSAV system. We then develop a set of numerical schemes which enjoy the same computational advantages as the SAV approach but can effectively handle both the volume and surface area constraints. In fact, these schemes are unconditionally energy stable and second-order accurate, and at each time step they can be decoupled into three fourth-order equations with constant coefficients, and each can be further reduced to two Poisson type equations. In particular, we also develop a time adaptive second-order scheme with the above properties. Thus, these schemes are easy to implement and extremely efficient, especially when coupled with a suitable adaptive time stepping.

The rest of the paper is organized as follows. We describe the PF-VMEM model with volume and surface area constraints in section 2. In section 3, we reformulate the PF-VMEM model into equivalent PDE systems by introducing two SAVs, develop a set of second-order, unconditionally energy stable schemes using the MSAV approach for the reformulated system, and show that they can be decoupled into three linear equations of fourth-order with only constant coefficients and are unconditionally energy stable. In section 4, we describe the MSAV approach in a general setting. In section 5, we present several numerical results to validate the accuracy and stability of the proposed schemes. Some concluding remarks are presented in section 6.

2. Vesicle membrane model. In the phase-field vesicle membrane model, the location of the membrane is described by a phase variable: $\phi(\boldsymbol{x}, t)$. The corresponding interface motion can be derived though the energetic approach with respect to the bending energy:

$$E_b(\phi) = \frac{\epsilon}{2}\int_\Omega \Big(-\Delta\phi + \frac{1}{\epsilon^2}G(\phi)\Big)^2 d\boldsymbol{x} = \frac{\epsilon}{2}\int_\Omega w^2 d\boldsymbol{x}, \tag{2.1}$$

where

$$w := -\Delta\phi + \frac{1}{\epsilon^2}G(\phi), \quad G(\phi) := F'(\phi),$$

where $F(\phi) = \frac{1}{4}(\phi^2-1)^2$ is the Ginzburg–Landau double well potential, and ϵ is the interfacial width. We define

$$A(\phi) = \int_\Omega (\phi+1)d\boldsymbol{x} \quad \textit{and} \quad B(\phi) = \int_\Omega \Big(\frac{\epsilon}{2}|\nabla\phi|^2 + \frac{1}{\epsilon}F(\phi)\Big)d\boldsymbol{x}. \tag{2.2}$$

Note that $\frac{1}{2}A(\phi)$ and $\frac{3}{2\sqrt{2}}B(\phi)$ represent the volume and surface area of the vesicle, respectively. In reality, the volume $A(\phi)$ and the surface area $B(\phi)$ of the vesicles do not change during the evolution in time. In order to numerically enforce these two constraints, we introduce two corresponding penalty terms in the free energy so that the total energy is

$$E_{tot}(\phi) = E_b(\phi) + \frac{1}{2\gamma}\Big(A(\phi)-\alpha\Big)^2 + \frac{1}{2\eta}\Big(B(\phi)-\beta\Big)^2, \tag{2.3}$$

where γ and η are two small parameters, and α, β represent the initial volume and surface area. Hence, the Allen–Cahn type dynamic equation takes the following form:

$$\phi_t = -M\mu, \tag{2.4}$$

$$\mu = -\epsilon\Delta w + \frac{1}{\epsilon}G'(\phi)w + \frac{1}{\gamma}\Big(A(\phi)-\alpha\Big) + \frac{1}{\eta}\Big(B(\phi)-\beta\Big)\Big(-\epsilon\Delta\phi + \frac{1}{\epsilon}F'(\phi)\Big), \tag{2.5}$$

$$w = -\Delta\phi + \frac{1}{\epsilon^2}G(\phi), \tag{2.6}$$

where M is the mobility constant. The boundary conditions can be either one of the following two types:

$$\text{(i) periodic or (ii) } \partial_{\mathbf{n}}\phi|_{\partial\Omega} = \partial_{\mathbf{n}}\mathrm{w}|_{\partial\Omega} = 0, \tag{2.7}$$

where $\mathbf{n}$ is the unit outward normal on the boundary $\partial\Omega$.

LEMMA 2.1. *The system* (2.4)–(2.6) *with* (2.7) *admits the following energy law:*

$$\frac{d}{dt}E_{tot}(\phi) = -M\|\mu\|^2, \tag{2.8}$$

where $\|\mu\|^2 = \int_\Omega \mu^2 d\boldsymbol{x}$.

Proof. By taking the L^2 inner product of (2.4) with μ, and of (2.5) with ϕ_t and of (2.6) with w, performing integration by parts, and summing up all the inequalities we obtain the energy law. ∎

3. Time discretization. We develop a set of second-order semidiscrete numerical schemes to solve the system (2.4)–(2.6). While we consider only time discretizations here, the results can carry over to any consistent finite-dimensional Galerkin approximations (finite elements or spectral) since the proof is based on variational formulations with all test functions in the same space as the trial function.

3.1. The SAV approach. The system (2.4)–(2.6) is highly nonlinear with three small parameters. A usual semi-implicit scheme, in which the nonlinear terms $G(\phi)$ and $B(\phi)$ are treated explicitly, will lead to a severe time step constraint, while treating nonlinear terms implicitly will result in a highly nonlinear system to solve at each time step. The recently proposed SAV approach [18] provides an effective way to construct unconditionally stable yet decoupled and linear schemes.

We first rewrite the original energy $E_b(\phi)$ as follows:

$$E_b(\phi) = \frac{\epsilon}{2}\int_\Omega \Big(-\Delta\phi + \frac{1}{\epsilon^2}G(\phi)\Big)^2 d\boldsymbol{x} = \frac{\epsilon}{2}\int_\Omega \Big(|\Delta\phi|^2 - \frac{2}{\epsilon^2}|\nabla\phi|^2 + \frac{6}{\epsilon^2}\phi^2|\nabla\phi|^2 + \frac{1}{\epsilon^4}(G(\phi))^2\Big)d\boldsymbol{x}. \tag{3.1}$$

In the SAV approach, we treat the first two linear terms in the above and the volume constraint term (which is also linear) implicitly and all other nonlinear terms explicitly. More precisely, letting $C > 0$ be a positive constant, we define a SAV

$$\tilde{V} = \sqrt{\int_\Omega \frac{\epsilon}{2}\Big(\frac{6}{\epsilon^2}\phi^2|\nabla\phi|^2 + \frac{1}{\epsilon^4}(G(\phi))^2\Big)d\boldsymbol{x} + \frac{1}{2\eta}(B(\phi)-\beta)^2 + C} \tag{3.2}$$

and rewrite the system (2.4)–(2.6) into the following equivalent system:

$$\phi_t = -M\mu, \tag{3.3}$$

$$\mu = \epsilon\Delta^2\phi + \frac{2}{\epsilon}\Delta\phi + \frac{1}{\gamma}(A(\phi)-\alpha) + 2\tilde{V}S(\phi), \tag{3.4}$$

$$\tilde{V}_t = \int_\Omega S(\phi)\phi_t d\boldsymbol{x}, \tag{3.5}$$

where $S(\phi) = \frac{\delta\tilde{V}}{\delta\phi}$. By taking the L^2 inner product of (3.3) with μ, of (3.4) with ϕ_t, and of (3.5) with $\tilde{V}$, we find that the new system satisfies the following energy dissipative law:

$$\frac{d}{dt}E(\phi;\tilde{V}) = -M\|\mu\|^2 \le 0, \tag{3.6}$$

where $E(\phi;\tilde{V}) = \frac{\epsilon}{2}\int_\Omega |\Delta\phi|^2 - \frac{2}{\epsilon^2}|\nabla\phi|^2 d\boldsymbol{x} + \tilde{V}^2 - C$ is a modified free energy which is equivalent to the original free energy in the time continuous case. Thus, one can use the general SAV approach developed in [18] to construct second-order, linear, decoupled, unconditionally energy stable schemes. As for all SAV schemes, they are very easy to implement. However, our numerical experiments indicate that the SAV schemes have difficulty enforcing the volume and surface area constraints unless exceedingly small time steps are used. In Figure 1, we consider the example in section 5.2 and plot the evolution of modified and original energies by using a second-order SAV scheme based on (3.3)–(3.5). We observe from Figure 1 that when $\eta = \gamma = 0.1$, both the modified energy and the original energy decay monotonically and the SAV scheme leads to a reasonable numerical solution. However, when $\eta = \gamma = 0.001$, while the modified energy still decays monotonically as it should, the corresponding original energy deviates significantly from the modified energy and the SAV scheme produces a nonphysical numerical solution even with a very small time step $\delta t = 0.00001$.

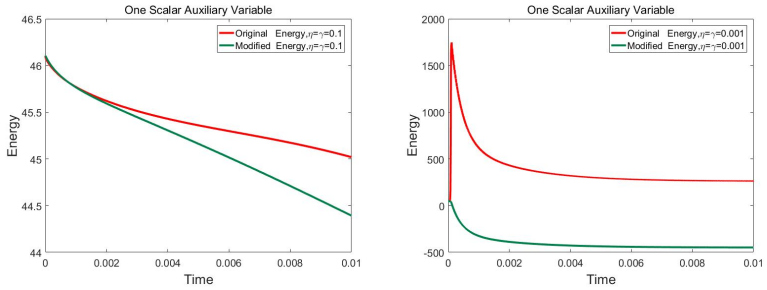

FIG. 1. *Evolution of the modified and original energies by the SAV scheme with* $\delta t = 0.00001$*: Left,* $\eta = \gamma = 0.1$*. Right:* $\eta = \gamma = 0.001$.

The main reason is that each of the two nonlinear terms in the total free energy has one small parameter and behaves differently, so a single SAV cannot adequately describe the two disparate evolution processes. Therefore it is natural to introduce two SAVs to reformulate the original system. We note that in [22] the authors also introduced multiple vector auxiliary variables in the IEQ framework, which results in coupled linear equations with variable coefficients to solve at each time step.

3.2. The MSAV approach. We introduce two new SAVs:

$$U(t) = B(\phi) - \beta, \qquad V(t) = \sqrt{\int_\Omega \Big(\frac{6}{\epsilon^2}\phi^2|\nabla\phi|^2 + \frac{1}{\epsilon^4}(G(\phi))^2\Big)d\boldsymbol{x} + C}, \tag{3.7}$$

where C is any positive constant to ensure $V(t) > 0$, so the total energy (2.3) becomes

$$E_{tot}(\phi; U, V) = \frac{\epsilon}{2}\int_\Omega \left(|\Delta\phi|^2 - \frac{2}{\epsilon^2}|\nabla\phi|^2\right) d\boldsymbol{x} + \frac{1}{2\gamma}(A(\phi) - \alpha)^2 + \frac{1}{2\eta}U^2 + \frac{\epsilon}{2}(V^2 - C), \tag{3.8}$$

and the system (2.4)–(2.6) becomes

$$\phi_t = -M\mu, \tag{3.9}$$

$$\mu = \frac{\delta E_{tot}}{\delta\phi} = \epsilon\Delta^2\phi + \frac{2}{\epsilon}\Delta\phi + \frac{1}{\gamma}(A(\phi) - \alpha) + \frac{1}{\eta}UH(\phi) + \epsilon VS(\phi), \tag{3.10}$$

$$U_t = \int_\Omega H(\phi)\phi_t d\boldsymbol{x}, \tag{3.11}$$

$$V_t = \int_\Omega S(\phi)\phi_t d\boldsymbol{x}, \tag{3.12}$$

where

$$S(\phi) = \frac{\delta V}{\delta\phi} = \frac{\frac{6}{\epsilon^2}\big(\phi|\nabla\phi|^2 - \nabla\cdot(\phi^2\nabla\phi)\big) + \frac{1}{\epsilon^4}G(\phi)G'(\phi)}{\sqrt{\int_\Omega \Big(\frac{6}{\epsilon^2}\phi^2|\nabla\phi|^2 + \frac{1}{\epsilon^4}(G(\phi))^2\Big)d\boldsymbol{x} + C}}, \tag{3.13}$$

$$H(\phi) = \frac{\delta U}{\delta\phi} = -\epsilon\Delta\phi + \frac{1}{\epsilon}F'(\phi). \tag{3.14}$$

The initial conditions are

$$\phi|_{t=0} = \phi^0, \quad U|_{t=0} = U(\phi^0), \quad V|_{t=0} = V(\phi^0), \tag{3.15}$$

and the boundary conditions are still (2.7).

The PDE system (3.9)–(3.12) is equivalent to the original system (2.4)–(2.6) and also admits an energy dissipative law. Indeed, by taking the L^2 inner product of (3.9) with μ, of (3.10) with ϕ_t, of (3.11) with U, and of (3.12) with V, performing integration by parts, and summing up all equalities, we obtain

$$\frac{d}{dt}E(\phi;U,V) = -M\|\mu\|^2 \le 0. \tag{3.16}$$

We first construct a second-order Crank–Nicolson scheme for (3.9)–(3.12).

Given $\delta t > 0$, let $t_n = n\delta t$. For any function $S(\cdot,t)$, S^n denotes a numerical approximation to $S(\cdot,t_n)$, and $S^{n+\frac{1}{2}} := \frac{S^{n+1}+S^n}{2}$.

Scheme 1 (MSAV-CN). Assuming that ϕ^{n-1}, ϕ^n, U^{n-1}, U^n, and V^{n-1}, V^n are known, we solve for ϕ^{n+1}, U^{n+1}, V^{n+1} as follows:

$$\frac{\phi^{n+1}-\phi^n}{\delta t} = -M\mu^{n+\frac{1}{2}}, \tag{3.17}$$

$$\begin{aligned}\mu^{n+\frac{1}{2}} = {}& \epsilon\Delta^2\phi^{n+\frac{1}{2}} + \frac{2}{\epsilon}\Delta\phi^{\star,n+\frac{1}{2}} \\ & + \frac{1}{\gamma}(A(\phi^{n+\frac{1}{2}})-\alpha) + \frac{1}{\eta}U^{n+\frac{1}{2}}H(\phi^{\star,n+\frac{1}{2}}) + \epsilon V^{n+\frac{1}{2}}S(\phi^{\star,n+\frac{1}{2}}),\end{aligned} \tag{3.18}$$

$$U^{n+1}-U^n = \int_\Omega H(\phi^{\star,n+\frac{1}{2}})(\phi^{n+1}-\phi^n)d\boldsymbol{x}, \tag{3.19}$$

$$V^{n+1}-V^n = \int_\Omega S(\phi^{\star,n+\frac{1}{2}})(\phi^{n+1}-\phi^n)d\boldsymbol{x}, \tag{3.20}$$

where $\phi^{\star,n+\frac{1}{2}} = \frac{3}{2}\phi^n - \frac{1}{2}\phi^{n-1}$ is a second-order extrapolation for $\phi^{n+\frac{1}{2}}$.

Note that in the above, we treated the linear term $\frac{2}{\epsilon}\Delta\phi^{\star,n+\frac{1}{2}}$. This is due to the fact that this linear term is negative definite so an implicit treatment will not help on the energy stability.

THEOREM 3.1. *The scheme* (3.17)–(3.20) *admits a unique solution and is unconditionally energy stable in the sense that it satisfies the following discrete energy dissipation law:*

$$E_{cn}^{n+1,n} - E_{cn}^{n,n-1} \le -\delta t M\|\mu^{n+\frac{1}{2}}\|^2, \tag{3.21}$$

where

$$\begin{aligned}E_{cn}^{n+1,n} = {}& \frac{\epsilon}{2}\|\Delta\phi^{n+1}\|^2 - \frac{1}{\epsilon}\|\nabla\phi^{n+1}\|^2 + \frac{1}{2\epsilon}\|\nabla\phi^{n+1}-\nabla\phi^n\|^2 \\ & + \frac{1}{2\eta}(U^{n+1})^2 + \frac{\epsilon}{2}(V^{n+1})^2 + \frac{1}{2\gamma}(A(\phi^{n+1})-\alpha)^2\end{aligned} \tag{3.22}$$

is the modified energy at t^{n+1}.

Proof. We first show that the scheme (3.17)–(3.20) admits a unique solution. To this end, we denote

$$B^{n+1} := \int_\Omega H^{\star,n+\frac{1}{2}}\phi^{n+1}d\boldsymbol{x},\ C^{n+1} := \int_\Omega S^{\star,n+\frac{1}{2}}\phi^{n+1}d\boldsymbol{x} \tag{3.23}$$

and rewrite (3.19) and (3.20) as

$$U^{n+1} = B^{n+1} + f^n,\ V^{n+1} = C^{n+1} + g^n \tag{3.24}$$

with $f^n = U^n - \int_\Omega H^{\star,n+\frac{1}{2}}\phi^n d\boldsymbol{x}$ and $g^n = V^n - \int_\Omega S^{\star,n+\frac{1}{2}}\phi^n d\boldsymbol{x}$. Then we can eliminate $U^{n+\frac{1}{2}}$ and $V^{n+\frac{1}{2}}$ from (3.18)–(3.20) to get

$$\left(\frac{1}{\delta t} + \frac{M\epsilon}{2}\Delta^2\right)\phi^{n+1} + \frac{M}{2\gamma}\int_\Omega \phi^{n+1}d\boldsymbol{x} + \frac{M}{2\eta}H^{\star,n+\frac{1}{2}}B^{n+1} + \frac{M\epsilon}{2}S^{\star,n+\frac{1}{2}}C^{n+1} = \tilde{f}^n, \tag{3.25}$$

where $\tilde{f}^n$ include all the explicit terms.

Next, we derive explicit formulas for computing B^{n+1} and C^{n+1}.

For any $f \in L^2(\Omega)$, we define a linear operator $\chi^{-1}(\cdot)$ in $L^2(\Omega)$ such that $\psi = \chi^{-1}(f)$ is the solution of

$$\left(\frac{1}{\delta t} + \frac{M\epsilon}{2}\Delta^2\right)\psi + \frac{M}{2\gamma}\int_\Omega \psi d\boldsymbol{x} = f \tag{3.26}$$

with the boundary conditions being

$$\text{(i) periodic or (ii) } \partial_{\mathbf{n}}\psi|_{\partial\Omega} = \partial_{\mathbf{n}}\Delta\psi|_{\partial\Omega} = 0. \tag{3.27}$$

Applying the operator χ^{-1} to (3.25), we obtain

$$\phi^{n+1} + \frac{M}{2\eta}\chi^{-1}(H^{\star,n+\frac{1}{2}})\,B^{n+1} + \frac{M\epsilon}{2}\chi^{-1}(S^{\star,n+\frac{1}{2}})\,C^{n+1} = \chi^{-1}(\tilde{f}^n). \tag{3.28}$$

Taking the L^2 inner product of (3.28) with $H^{\star,n+\frac{1}{2}}$, we find

$$\left(1 + \frac{M}{2\eta}(H^{\star,n+\frac{1}{2}}, \chi^{-1}(H^{\star,n+\frac{1}{2}}))\right)B^{n+1} + \frac{M\epsilon}{2}(H^{\star,n+\frac{1}{2}}, \chi^{-1}(S^{\star,n+\frac{1}{2}}))\,C^{n+1} = (H^{\star,n+\frac{1}{2}}, \chi^{-1}(\tilde{f}^n)). \tag{3.29}$$

Taking the L^2 inner product of (3.28) with $S^{\star,n+\frac{1}{2}}$, we find

$$\frac{M}{2\eta}(S^{\star,n+\frac{1}{2}}, \chi^{-1}(H^{\star,n+\frac{1}{2}}))\,B^{n+1} + \left(1 + \frac{M\epsilon}{2}(S^{\star,n+\frac{1}{2}}, \chi^{-1}(S^{\star,n+\frac{1}{2}}))\right)C^{n+1} = (S^{\star,n+\frac{1}{2}}, \chi^{-1}(\tilde{f}^n)). \tag{3.30}$$

The above two equations form a 2×2 linear system for the unknowns $(B^{n+1}, C^{n+1})^t$. It remains to shown that the 2×2 matrix

$$D = \begin{pmatrix} 1 + \frac{M}{2\eta}(H^{\star,n+\frac{1}{2}}, \chi^{-1}(H^{\star,n+\frac{1}{2}})) & \frac{M\epsilon}{2}(H^{\star,n+\frac{1}{2}}, \chi^{-1}(S^{\star,n+\frac{1}{2}})) \\ \frac{M}{2\eta}(S^{\star,n+\frac{1}{2}}, \chi^{-1}(H^{\star,n+\frac{1}{2}})) & 1 + \frac{M\epsilon}{2}(S^{\star,n+\frac{1}{2}}, \chi^{-1}(S^{\star,n+\frac{1}{2}})) \end{pmatrix}$$

is nonsingular.

It is clear that $(H^{\star,n+\frac{1}{2}}, \chi^{-1}(H^{\star,n+\frac{1}{2}})) \geq 0$ and $(S^{\star,n+\frac{1}{2}}, \chi^{-1}(S^{\star,n+\frac{1}{2}})) \geq 0$. Using the Cauchy–Schwarz inequality and integration by parts, we obtain

$$\begin{aligned} &(H^{\star,n+\frac{1}{2}}, \chi^{-1}(S^{\star,n+\frac{1}{2}})) = (\chi^{-\frac{1}{2}}H^{\star,n+\frac{1}{2}}, \chi^{-\frac{1}{2}}(S^{\star,n+\frac{1}{2}})) \\ &\leq (\chi^{-\frac{1}{2}}H^{\star,n+\frac{1}{2}}, \chi^{-\frac{1}{2}}H^{\star,n+\frac{1}{2}})^{\frac{1}{2}}(\chi^{-\frac{1}{2}}S^{\star,n+\frac{1}{2}}, \chi^{-\frac{1}{2}}S^{\star,n+\frac{1}{2}})^{\frac{1}{2}} \\ &= (H^{\star,n+\frac{1}{2}}, \chi^{-1}H^{\star,n+\frac{1}{2}})^{\frac{1}{2}}(S^{\star,n+\frac{1}{2}}, \chi^{-1}S^{\star,n+\frac{1}{2}})^{\frac{1}{2}}. \end{aligned} \tag{3.31}$$

Similarly, we have

$$
\begin{aligned}
&(S^{\star,n+\frac{1}{2}}, \chi^{-1}(H^{\star,n+\frac{1}{2}})) = (\chi^{-\frac{1}{2}} H^{\star,n+\frac{1}{2}}, \chi^{-\frac{1}{2}}(S^{\star,n+\frac{1}{2}}))\\
&\le (\chi^{-\frac{1}{2}} H^{\star,n+\frac{1}{2}}, \chi^{-\frac{1}{2}} H^{\star,n+\frac{1}{2}})^{\frac{1}{2}} (\chi^{-\frac{1}{2}} S^{\star,n+\frac{1}{2}}, \chi^{-\frac{1}{2}} S^{\star,n+\frac{1}{2}})^{\frac{1}{2}}\\
&= (H^{\star,n+\frac{1}{2}}, \chi^{-1} H^{\star,n+\frac{1}{2}})^{\frac{1}{2}} (S^{\star,n+\frac{1}{2}}, \chi^{-1} S^{\star,n+\frac{1}{2}})^{\frac{1}{2}}.
\end{aligned} \tag{3.32}
$$

We derive from the above that the determinant of D is positive so the system (3.29)–(3.30) admits a unique solution $(B^{n+1}, C^{n+1})^t$. Then ϕ^{n+1} is uniquely determined from (3.28).

Next, we show the scheme is unconditionally energy stable. Taking the L^2 inner product of (3.17) with $\delta t \mu^{n+\frac{1}{2}}$, we obtain

$$
(\phi^{n+1} - \phi^n, \mu^{n+\frac{1}{2}}) = -\delta t M \|\mu^{n+\frac{1}{2}}\|^2. \tag{3.33}
$$

Taking the L^2 inner product of (3.18) with $\phi^{n+1} - \phi^n$, we derive

$$
\begin{aligned}
(\mu^{n+\frac{1}{2}}, \phi^{n+1} - \phi^n) &= (\epsilon \Delta^2 \phi^{n+\frac{1}{2}}, \phi^{n+1} - \phi^n) + \left(\frac{2}{\epsilon} \Delta \phi^{\star,n+\frac{1}{2}}, \phi^{n+1} - \phi^n\right)\\
&+ \frac{1}{\gamma}\left(A(\phi^{n+\frac{1}{2}}) - \alpha, \phi^{n+1} - \phi^n\right) + \left(\frac{1}{\eta} U^{n+\frac{1}{2}} H(\phi^{\star,n+\frac{1}{2}}), \phi^{n+1} - \phi^n\right)\\
&+ (\epsilon V^{n+\frac{1}{2}} S(\phi^{\star,n+\frac{1}{2}}), \phi^{n+1} - \phi^n).
\end{aligned} \tag{3.34}
$$

Taking the L^2 inner product of (3.19) with $U^{n+\frac{1}{2}}$ and of (3.20) with $V^{n+\frac{1}{2}}$, we obtain respectively

$$
\frac{1}{2}((U^{n+1})^2 - (U^n)^2) = \int_\Omega U^{n+\frac{1}{2}} H(\phi^{\star,n+\frac{1}{2}})(\phi^{n+1} - \phi^n) d\boldsymbol{x}, \tag{3.35}
$$

$$
\frac{1}{2}((V^{n+1})^2 - (V^n)^2) = \int_\Omega V^{n+\frac{1}{2}} S(\phi^{\star,n+\frac{1}{2}})(\phi^{n+1} - \phi^n) d\boldsymbol{x}. \tag{3.36}
$$

Using the equality

$$
\frac{1}{2}(3b - c, a - b) = \frac{1}{2}(|a|^2 - |b|^2) - \frac{1}{4}(|a - b|^2 - |b - c|^2 + |a - 2b + c|^2), \tag{3.37}
$$

we derive from integration by parts that

$$
\begin{aligned}
(\Delta \phi^{\star,n+\frac{1}{2}}, \phi^{n+1} - \phi^n) &= -\frac{1}{2}(\|\nabla \phi^{n+1}\|^2 - \|\nabla \phi^n\|^2) + \frac{1}{4}(\|\nabla \phi^{n+1} - \nabla \phi^n\|^2\\
&- \|\nabla \phi^n - \nabla \phi^{n-1}\|^2 + \|\nabla \phi^{n+1} - 2\nabla \phi^n + \nabla \phi^{n-1}\|^2).
\end{aligned} \tag{3.38}
$$

Combining (3.34)–(3.36) and (3.38), we obtain

$$
\begin{aligned}
(\mu^{n+\frac{1}{2}}, \phi^{n+1} - \phi^n) =& \frac{\epsilon}{2}(\|\Delta \phi^{n+1}\|^2 - \|\Delta \phi^n\|^2) - \frac{1}{\epsilon}(\|\nabla \phi^{n+1}\|^2 - \|\nabla \phi^n\|^2)\\
&+ \frac{1}{2\epsilon}(\|\nabla \phi^{n+1} - \nabla \phi^n\|^2 - \|\nabla \phi^n - \nabla \phi^{n-1}\|^2\\
&+ \|\nabla \phi^{n+1} - 2\nabla \phi^n + \nabla \phi^{n-1}\|^2)\\
&+ \frac{1}{2\gamma}\left((A(\phi^{n+1}) - \alpha)^2 - (A(\phi^n) - \alpha)^2\right)\\
&+ \frac{1}{2\eta}\left((U^{n+1})^2 - (U^n)^2\right)\\
&+ \frac{\epsilon}{2}\left((V^{n+1})^2 - (V^n)^2\right).
\end{aligned}
$$

Finally, combining the above with (3.33) and dropping some positive terms, we obtain the following energy dissipative law:

$$\begin{aligned}&\Big(\frac{\epsilon}{2}\|\Delta\phi^{n+1}\|^2-\frac{1}{\epsilon}\|\nabla\phi^{n+1}\|^2+\frac{1}{2\epsilon}\|\nabla\phi^{n+1}-\nabla\phi^n\|^2\\&+\frac{1}{2\gamma}\big(A(\phi^{n+1})-\alpha\big)^2+\frac{1}{2\eta}(U^{n+1})^2+\frac{\epsilon}{2}(V^{n+1})^2\Big)\\&-\Big(\frac{\epsilon}{2}\|\Delta\phi^{n}\|^2-\frac{1}{\epsilon}\|\nabla\phi^{n}\|^2+\frac{1}{2\epsilon}\|\nabla\phi^{n}-\nabla\phi^{n-1}\|^2\\&+\frac{1}{2\gamma}\big(A(\phi^{n})-\alpha\big)^2+\frac{1}{2\eta}(U^{n})^2+\frac{\epsilon}{2}(V^{n})^2\Big)\le-\delta tM\|\mu^{n+\frac12}\|^2.\end{aligned}$$

Then proof is complete. ∎

Remark 3.1. In summary, at each time step of Scheme 1, we need to

1. compute $\chi^{-1}(H^{\star,n+\frac12})$, $\chi^{-1}(S^{\star,n+\frac12})$, $\chi^{-1}(\tilde f^n)$ which require solving three decoupled equations of the form (3.26) with the boundary conditions (3.27);
2. solve $(B^{n+1},C^{n+1})^t$ from the 2×2 linear system (3.29)–(3.30);
3. update ϕ^{n+1} from (3.28).

Taking the integral of (3.26) over Ω, thanks to (3.27), we find immediately that $(\frac{1}{\delta t}+\frac{M|\Omega|}{2\gamma})\int_\Omega\phi d\boldsymbol{x}=\int_\Omega f d\boldsymbol{x}$. Hence, (3.26) reduces to a usual fourth-order equation with (3.27), which can be further reduced to two decoupled Poisson type equations [23]. Therefore, Scheme 1 is extremely efficient and easy to implement.

Remark 3.2. Note that an additional vector auxiliary variable is introduced in [22] to enforce the volume constraint. However, since this constraint leads to a linear term in (2.5), it is advantageous to treat it implicitly since it is more accurate and computationally more efficient as it requires solving only three fourth-order equations instead of four if additional SAV is introduced.

Another way to construct efficient schemes using the SAV or MSAV approach is through the backward differentiation formulas. Below is a second-order version.

Scheme 2 (MSAV-BDF2). Assuming that ϕ^{n-1}, ϕ^n, U^{n-1}, U^n, and V^{n-1}, V^n are known, we solve ϕ^{n+1}, U^{n+1}, and V^{n+1} as follows:

$$\frac{3\phi^{n+1}-4\phi^n+\phi^{n-1}}{2\delta t}=-M\mu^{n+1},\tag{3.39}$$

$$\begin{aligned}\mu^{n+1}=\epsilon\Delta^2\phi^{n+1}+\frac{2}{\epsilon}\Delta\phi^{\dagger,n+1}+\frac{1}{\gamma}(A(\phi^{n+1})-\alpha)\\+\frac{1}{\eta}U^{n+1}H(\phi^{\dagger,n+1})+\epsilon V^{n+1}S(\phi^{\dagger,n+1}),\end{aligned}\tag{3.40}$$

$$3U^{n+1}-4U^n+U^{n-1}=\int_\Omega H(\phi^{\dagger,n+1})(3\phi^{n+1}-4\phi^n+\phi^{n-1})d\boldsymbol{x},\tag{3.41}$$

$$3V^{n+1}-4V^n+V^{n-1}=\int_\Omega S(\phi^{\dagger,n+1})(3\phi^{n+1}-4\phi^n+\phi^{n-1})d\boldsymbol{x}.\tag{3.42}$$

where $\phi^{\dagger,n+1}=2\phi^n-\phi^{n-1}$. The boundary conditions are still (2.7).

This scheme possesses the same nice properties as Scheme 1 and, at each time step, can also be decoupled into three linear, constant coefficient fourth-order equations.

THEOREM 3.2. *The scheme* (3.39)–(3.42) *admits a unique solution and is unconditionally energy stable, i.e., satisfies the following discrete energy dissipation law:*

$$E_{bdf2}^{n+1,n} - E_{bdf2}^{n,n-1} \le -2\delta t M \|\mu^{n+1}\|^2, \tag{3.43}$$

where

$$\begin{aligned} E_{bdf2}^{n+1,n} =& \frac{\epsilon}{2}(\|\Delta\phi^{n+1}\|^2 + \|2\Delta\phi^{n+1} - \Delta\phi^n\|^2) - \frac{1}{\epsilon}(\|\nabla\phi^{n+1}\|^2 \\ &+ \|2\nabla\phi^{n+1} - \nabla\phi^n\|^2 - 2\|\nabla\phi^{n+1} - \nabla\phi^n\|^2) \\ &+ \frac{1}{2\gamma}\Big((A(\phi^{n+1}) - \alpha)^2 - (2A(\phi^{n+1}) - A(\phi^n) - \alpha)^2\Big) \\ &+ \frac{1}{2\eta}\Big((U^{n+1})^2 - (2U^{n+1} - U^n)^2\Big) \\ &+ \frac{\epsilon}{2}\Big((V^{n+1})^2 - (2V^{n+1} - V^n)^2\Big). \end{aligned} \tag{3.44}$$

Proof. The proof for the existence of a unique solution is essentially the same as for Scheme 1 so we shall only prove its stability.

Taking the L^2 inner product of (3.39) with $2\delta t\mu^{n+1}$, we obtain

$$(3\phi^{n+1} - 4\phi^n + \phi^{n-1}, \mu^{n+1}) = -2\delta t M\|\mu^{n+1}\|^2. \tag{3.45}$$

Taking the L^2 inner product of (3.40) with $3\phi^{n+1} - 4\phi^n + \phi^{n-1}$, we have

$$\begin{aligned} (\mu^{n+1}, 3\phi^{n+1} - 4\phi^n + \phi^{n-1}) =& (\epsilon\Delta^2\phi^{n+1}, 3\phi^{n+1} - 4\phi^n + \phi^{n-1}) \\ &+ \left(\frac{2}{\epsilon}\Delta\phi^{\dagger,n+1}, 3\phi^{n+1} - 4\phi^n + \phi^{n-1}\right) \\ &+ \frac{1}{\gamma}\Big(A(\phi^{n+1}) - \alpha, 3\phi^{n+1} - 4\phi^n + \phi^{n-1}\Big) \\ &+ \left(\frac{1}{\eta}U^{n+1}H(\phi^{\dagger,n+1}), 3\phi^{n+1} - 4\phi^n + \phi^{n-1}\right) \\ &+ (\epsilon V^{n+\frac{1}{2}}S(\phi^{\dagger,n+1}), 3\phi^{n+1} - 4\phi^n + \phi^{n-1}), \end{aligned} \tag{3.46}$$

Taking the L^2 inner product of (3.41) with $2U^{n+1}$ and of (3.42) with $2V^{n+1}$, and using the equality

$$2(3a - 4b + c, a) = |a|^2 - |b|^2 + |2a - b|^2 - |2b - c|^2 + |a - 2b + c|^2, \tag{3.47}$$

we obtain respectively

$$\begin{aligned} \frac{1}{\gamma}((A(\phi^{n+1}) - \alpha), 3\phi^{n+1} - 4\phi^n + \phi^{n-1}) =& \frac{1}{2\gamma}((A(\phi^{n+1}) - \alpha)^2 - (A(\phi^n) - \alpha)^2) \\ &+ \frac{1}{2\gamma}((2A(\phi^{n+1}) - A(\phi^n) - \alpha)^2 - (2A(\phi^n) - A(\phi^{n-1}) - \alpha)^2) \\ &+ \frac{1}{2\gamma}(A(\phi^{n+1}) - 2A(\phi^n) + A(\phi^{n-1}))^2, \end{aligned} \tag{3.48}$$

$$\begin{aligned} &(|U^{n+1}|^2 - |U^n|^2 + |2U^{n+1} - U^n|^2 - |2U^n - U^{n-1}|^2 + |U^{n+1} - 2U^n + U^{n-1}|^2) \\ &\qquad = \int_\Omega 2U^{n+1}H(\phi^{\dagger,n+1})(3\phi^{n+1} - 4\phi^n + \phi^{n-1})d\boldsymbol{x}, \end{aligned} \tag{3.49}$$

and

$$(|V^{n+1}|^2-|V^n|^2+|2V^{n+1}-V^n|^2-|2V^n-V^{n-1}|^2+|V^{n+1}-2V^n+V^{n-1}|^2) = \int_\Omega 2V^{n+1}S(\phi^{\dagger,n+1})(3\phi^{n+1}-4\phi^n+\phi^{n-1})d\boldsymbol{x}, \tag{3.50}$$

Using the equality

$$\begin{aligned} 2(3a-4b+c,2b-c) &= (|a|^2+|2a-b|^2-2|a-b|^2) \\ &\quad -(|b|^2+|2b-c|^2-2|b-c|^2)-3|a-2b+c|^2, \end{aligned} \tag{3.51}$$

and taking integration by parts, we obtain

$$\begin{aligned} -2(\Delta\phi^{\dagger,n+1},3\phi^{n+1}-4\phi^n+\phi^{n-1}) &= (\|\nabla\phi^{n+1}\|^2+\|2\nabla\phi^{n+1}-\nabla\phi^n\|^2-2\|\nabla\phi^{n+1}-\nabla\phi^n\|^2) \\ &\quad -(\|\nabla\phi^n\|^2+\|2\nabla\phi^n-\nabla\phi^{n-1}\|^2-2\|\nabla\phi^n-\nabla\phi^{n-1}\|^2) \\ &\quad -3\|\nabla\phi^{n+1}-2\nabla\phi^n+\nabla\phi^{n-1}\|^2. \end{aligned} \tag{3.52}$$

By using the equality (3.47), we know that

$$\begin{aligned} (2\Delta^2\phi^{n+1},3\phi^{n+1}-4\phi^n+\phi^{n-1}) &= \|\Delta\phi^{n+1}\|^2-\|\Delta\phi^n\|^2 \\ &\quad +\|2\Delta\phi^{n+1}-\Delta\phi^n\|^2-\|2\Delta\phi^n-\Delta\phi^{n-1}\|^2 \\ &\quad +\|\Delta\phi^{n+1}-2\Delta\phi^n+\Delta\phi^{n-1}\|^2. \end{aligned} \tag{3.53}$$

Combining (3.45) to (3.53) leads to

$$\begin{aligned} &(\mu^{n+1},3\phi^{n+1}-4\phi^n+\phi^{n-1}) = \frac{\epsilon}{2}(\|\Delta\phi^{n+1}\|^2+\|2\Delta\phi^{n+1}-\Delta\phi^n\|^2) \\ &-\frac{\epsilon}{2}(\|\Delta\phi^n\|^2+\|2\Delta\phi^n-\Delta\phi^{n-1}\|^2)+\frac{\epsilon}{2}\|\Delta\phi^{n+1}-2\Delta\phi^n+\Delta\phi^{n-1}\|^2 \\ &-\frac{1}{\epsilon}(\|\nabla\phi^{n+1}\|^2+\|2\nabla\phi^{n+1}-\nabla\phi^n\|^2-2\|\nabla\phi^{n+1}-\nabla\phi^n\|^2) \\ &+\frac{1}{\epsilon}(\|\nabla\phi^n\|^2+\|2\nabla\phi^n-\nabla\phi^{n-1}\|^2-2\|\nabla\phi^n-\nabla\phi^{n-1}\|^2) \\ &+\frac{3}{\epsilon}\|\nabla\phi^{n+1}-2\nabla\phi^n+\nabla\phi^{n-1}\|^2+\frac{1}{2\gamma}(A(\phi^{n+1})-2A(\phi^n)+A(\phi^{n-1}))^2 \\ &+\frac{1}{2\eta}\Big((U^{n+1})^2-(U^n)^2+(2U^{n+1}-U^n)^2-(2U^n-U^{n-1})^2+(U^{n+1}-2U^n+U^{n-1})^2\Big) \\ &+\frac{\epsilon}{2}\Big((V^{n+1})^2-(V^n)^2+(2V^{n+1}-V^n)^2-(2V^n-V^{n-1})^2+(V^{n+1}-2V^n+V^{n-1})^2\Big) \\ &+\frac{1}{2\gamma}\Big((A(\phi^{n+1})-\alpha)^2-(A(\phi^n)-\alpha)^2+(2A(\phi^{n+1}) \\ &-A(\phi^n)-\alpha)^2-(2A(\phi^n)-A(\phi^{n-1})-\alpha)^2\Big). \end{aligned}$$

Finally, combining the last inequality with (3.45) and dropping some positive terms, we obtain the desired result. ∎

3.3. A second-order scheme with adaptive time stepping. In many applications, energy evolution may undergo large variations initially and at some time intervals, but may change very little in some other time intervals (see, e.g., simulations in the next subsection). One main advantage of unconditionally energy stable

schemes is that they can be easily combined with an adaptive strategy which chooses time steps based on the accuracy requirement only. So small time steps are only used when the energy variation is large, while larger time steps can be used when the energy variation is small.

While it is straightforward to apply variable time steps to first-order schemes without affecting the unconditional stability, it is generally nontrivial to preserve unconditional stability for second-order schemes with variable time steps, except for the fully implicit Crank–Nicolson scheme. In fact, both Scheme 1 and Scheme 2 cannot preserve the unconditional stability with variable time steps. Below, we construct an unconditionally stable, second-order scheme with variable time steps by modifying Scheme 1 slightly.

Let $\{t_n\}$ be an increasing sequence with $t_0 = 0$, and set $\delta t_n = t_{n+1} - t_n$.

Scheme 3 (MSAV-CN2). Assuming that ϕ^{n-1}, ϕ^n, U^{n-1}, U^n, and V^{n-1}, V^n are known, we solve for ϕ^{n+1}, U^{n+1}, V^{n+1} as follows:

$$\frac{\phi^{n+1} - \phi^n}{\delta t_n} = -M\mu^{n+\frac{1}{2}}, \tag{3.54}$$

$$\begin{aligned}\mu^{n+\frac{1}{2}} = {} & \epsilon\Delta^2\phi^{n+\frac{1}{2}} + \frac{2}{\epsilon}\Delta\phi^{n+\frac{1}{2}} \\ & + \frac{1}{\gamma}(A(\phi^{n+\frac{1}{2}}) - \alpha) + \frac{1}{\eta}U^{n+\frac{1}{2}}H(\phi^{\star,n+\frac{1}{2}}) + \epsilon V^{n+\frac{1}{2}}S(\phi^{\star,n+\frac{1}{2}}),\end{aligned} \tag{3.55}$$

$$U^{n+1} - U^n = \int_\Omega H(\phi^{\star,n+\frac{1}{2}})(\phi^{n+1} - \phi^n)d\boldsymbol{x}, \tag{3.56}$$

$$V^{n+1} - V^n = \int_\Omega S(\phi^{\star,n+\frac{1}{2}})(\phi^{n+1} - \phi^n)d\boldsymbol{x}, \tag{3.57}$$

where $\phi^{\star,n+\frac{1}{2}} = (\frac{\delta t_n}{2\delta t_{n-1}} + 1)\phi^n - \frac{\delta t_n}{2\delta t_{n-1}}\phi^{n-1}$ is a second-order extrapolation for $\phi^{n+\frac{1}{2}}$.

Note that besides variable time steps, the only other difference between the above scheme and Scheme 1 is that we replaced the explicit $\Delta\phi^{\star,n+\frac{1}{2}}$ in (3.18) by the implicit $\Delta\phi^{n+\frac{1}{2}}$ in (3.55). Like Scheme 1, it can still be decoupled into three fourth-order equations at each time step.

THEOREM 3.3. *The scheme* (3.54)–(3.57) *is unconditionally energy stable in the sense that it satisfies the following discrete energy dissipation law:*

$$E_{cn2}^{n+1,n} - E_{cn2}^{n,n-1} \le -\delta t_n M\|\mu^{n+\frac{1}{2}}\|^2, \tag{3.58}$$

where

$$\begin{aligned}E_{cn2}^{n+1,n} = {} & \frac{\epsilon}{2}\|\Delta\phi^{n+1}\|^2 - \frac{1}{\epsilon}\|\nabla\phi^{n+1}\|^2 \\ & + \frac{1}{2\eta}(U^{n+1})^2 + \frac{\epsilon}{2}(V^{n+1})^2 + \frac{1}{2\gamma}(A(\phi^{n+1}) - \alpha)^2\end{aligned} \tag{3.59}$$

is the modified energy at t^{n+1}.

Proof. The proof is quite similar to that of Theorem 3.1.

Taking the L^2 inner product of (3.54) with $\delta t_n\mu^{n+\frac{1}{2}}$, we obtain

$$(\phi^{n+1} - \phi^n, \mu^{n+\frac{1}{2}}) = -\delta t_n M\|\mu^{n+\frac{1}{2}}\|^2. \tag{3.60}$$

Taking the L^2 inner product of (3.55) with $\phi^{n+1}-\phi^n$ and integrating by parts, we derive

$$
\begin{aligned}
(\mu^{n+\frac{1}{2}},\phi^{n+1}-\phi^n) &= \frac{\epsilon}{2}(\|\Delta\phi^{n+1}\|^2-\|\Delta\phi^n\|^2)-\frac{1}{\epsilon}(\|\nabla\phi^{n+1}\|^2-\|\nabla\phi^n\|^2)\\
&+\frac{1}{\gamma}\Big(A(\phi^{n+\frac{1}{2}}-\alpha),\phi^{n+1}-\phi^n\Big)+\Big(\frac{1}{\eta}U^{n+\frac{1}{2}}H(\phi^{\star,n+\frac{1}{2}}),\phi^{n+1}-\phi^n\Big)\\
&+(\epsilon V^{n+\frac{1}{2}}S(\phi^{\star,n+\frac{1}{2}}),\phi^{n+1}-\phi^n).
\end{aligned}
\tag{3.61}
$$

Taking the L^2 inner product of (3.56) with $U^{n+\frac{1}{2}}$, of (3.57) with $V^{n+\frac{1}{2}}$, we obtain respectively

$$
\frac{1}{2}((U^{n+1})^2-(U^n)^2)=\int_\Omega U^{n+\frac{1}{2}}H(\phi^{\star,n+\frac{1}{2}})(\phi^{n+1}-\phi^n)d\boldsymbol{x},
\tag{3.62}
$$

$$
\frac{1}{2}((V^{n+1})^2-(V^n)^2)=\int_\Omega V^{n+\frac{1}{2}}S(\phi^{\star,n+\frac{1}{2}})(\phi^{n+1}-\phi^n)d\boldsymbol{x}.
\tag{3.63}
$$

Combining (3.61)–(3.63), we obtain

$$
\begin{aligned}
(\mu^{n+\frac{1}{2}},\phi^{n+1}-\phi^n) &= \frac{\epsilon}{2}(\|\Delta\phi^{n+1}\|^2-\|\Delta\phi^n\|^2)-\frac{1}{\epsilon}(\|\nabla\phi^{n+1}\|^2-\|\nabla\phi^n\|^2)\\
&+\frac{1}{2\gamma}\Big((A(\phi^{n+1})-\alpha)^2-(A(\phi^n)-\alpha)^2\Big)+\frac{1}{2\eta}\Big((U^{n+1})^2-(U^n)^2\Big)\\
&+\frac{\epsilon}{2}\Big((V^{n+1})^2-(V^n)^2\Big).
\end{aligned}
$$

We obtain the desired result from the above and (3.60). ∎

One simple but effective strategy is to update the time step size by using the formula [9, 15]

$$
A_{dp}(e,\tau)=\rho\left(\frac{tol}{e}\right)^{\frac{1}{2}}\tau,
\tag{3.64}
$$

where e is a relative error, τ is the time step, *tol* is the error tolerance, and ρ is a parameter. One can of course use other adaptive strategies such as those in [14].

A second-order adaptive time step algorithm based on Scheme 3 is given below.

Algorithm 1. *Adaptive time stepping with Scheme* 3.

Given *Solutions at time steps n and $n-1$; parameter tol and ρ, and the preassigned minimum and maximin allowable time steps δt_{min} and δt_{max}.*

Step 1 *Compute $(\phi_1,U_1,V_1)^{n+1}$ by the first-order MSAV scheme with δt^n.*

Step 2 *Compute $(\phi_2,U_2,V_2)^{n+1}$ by Scheme* 3 *with δt^n.*

Step 3 *Calculate* $e_{n+1}=\max\{\frac{\|U_2^{n+1}-U_1^{n+1}\|}{\|U_2^{n+1}\|},\frac{\|V_2^{n+1}-V_1^{n+1}\|}{\|V_2^{n+1}\|},\frac{\|\phi_2^{n+1}-\phi_1^{n+1}\|}{\|\phi_2^{n+1}\|}\}$.

Step 4 ***if*** $e_{n+1}>tol$, ***then***

Recalculate time step $\delta t^n\leftarrow\max\{\delta t_{min},\min\{A_{dp}(e_{n+1},\delta t^n),\delta t_{max}\}\}$.

Step 5 ***goto*** *Step* 1

Step 6 ***else***

Update time step $\delta t^{n+1}\leftarrow\max\{\delta t_{min},\min\{A_{dp}(e_{n+1},\delta t^n),\delta t_{max}\}\}$.

Step 7 ***endif***

4. MSAV approach in a general setting. We present in this section the MSAV approach in a more general setting. Consider, for instance, the free energy:

$$E(\phi) = \int_\Omega \left[\frac{1}{2}\phi\,\mathcal{L}\phi + \sum_{i=1}^{k} \frac{1}{\epsilon_i} F_i(\phi) \right] d\boldsymbol{x}, \tag{4.1}$$

where $\mathcal{L}$ is a linear elliptic operator and $\{F_i(\phi)\}$ are different nonlinear potentials and $\{\epsilon_i\}$ are possibly small parameters. We consider the following gradient flow:

$$\begin{aligned} &\frac{\partial \phi}{\partial t} = -\mathcal{G}\mu, \\ &\mu := \frac{\delta E}{\delta \phi} = \mathcal{L}\phi + \sum_{i=1}^{k} \frac{1}{\epsilon_i} F_i'(\phi), \end{aligned} \tag{4.2}$$

where $\mathcal{G}$ is a positive definite operator, e.g., $\mathcal{G} = I$ is the L^2 gradient flow and $\mathcal{G} = -\Delta$ is the so-called H^{-1} gradient flow. Due to the disparate nonlinear terms, it may not be effective to use one single SAV to deal with all nonlinear terms, so we introduce one SAV for each disparate nonlinear potential in the free energy.

Assuming $E_i(\phi)=\int_\Omega \frac{1}{\epsilon_i} F_i(\phi) dx > -C_i$ $(C_i > 0)$, we introduce $r_i(t)=\sqrt{E_i(\phi)+C_i}$, $i = 1, \ldots, k$ and rewrite the free energy as

$$E(\phi) = \int_\Omega \left[\frac{1}{2}\phi\,\mathcal{L}\phi + \sum_{i=1}^{k} (r_i^2(t) - C_i) \right] d\boldsymbol{x}. \tag{4.3}$$

Then, we can write an equivalent gradient flow based on the above free energy as follows:

$$\begin{aligned} &\frac{\partial \phi}{\partial t} = -\mathcal{G}\mu, \\ &\mu = \mathcal{L}\phi + \sum_{i=1}^{k} 2 r_i(t) \frac{\delta E_i}{\delta \phi}, \\ &\partial_t r_i = \int_\Omega \frac{\delta E_i}{\delta \phi} \phi_t dx, \quad i = 1, \ldots, k. \end{aligned} \tag{4.4}$$

For any sequence $\{g^n\}$, we denote $g^{n+1/2} = \frac{g^{n+1}+g^n}{2}$ and $g^{*,n+1/2} = \frac{3}{2}g^n - \frac{1}{2}g^{n-1}$. Then, a second-order MSAV scheme based on Crank–Nicolson and Adams–Bashforth is as follows:

$$\begin{aligned} &\frac{\phi^{n+1} - \phi^n}{\Delta t} = -\mathcal{G}\mu^{n+1/2}, \\ &\mu^{n+1/2} = \mathcal{L}\phi^{n+1/2} + \sum_{i=1}^{k} 2 r_i^{n+1/2} \frac{\delta E_i}{\delta \phi}^{*,n+1/2}, \\ &r_i^{n+1} - r_i^n = \int_\Omega \frac{\delta E_i}{\delta \phi}^{*,n+1/2} (\phi^{n+1} - \phi^n)\, dx, \quad i = 1, \ldots, k. \end{aligned} \tag{4.5}$$

THEOREM 4.1. *The scheme* (4.5) *is linear, second-order accurate, uniquely solvable, and unconditionally energy stable in the following sense:*

$$\Big[\frac{1}{2}(\mathcal{L}\phi^{n+1},\phi^{n+1})+\sum_{i=1}^{k}(r_i^{n+1})^2\Big]-\Big[\frac{1}{2}(\mathcal{L}\phi^{n},\phi^{n})+\sum_{i=1}^{k}(r_i^{n})^2\Big]=-\Delta t\|\nabla\mu^{n+1/2}\|^2. \tag{4.6}$$

Proof. It is clear that the scheme (4.5) is linear and second-order accurate. Taking the inner product of the equations in (4.5) successively with $\Delta t\mu^{n+1/2}$, $\phi^{n+1}-\phi^n$, and $2r_i^{n+1/2}$ $(i=1,\dots,k)$ and summing up the results, we obtain immediately (4.6). The unique solvability is just a direct consequence of (4.6). ∎

Next we show that the scheme (4.5) can be efficiently solved. Indeed, we can write it as a matrix system

$$\begin{pmatrix} \frac{1}{\Delta t}I & \mathcal{G} & 0\\ -\mathcal{L} & I & *\\ * & 0 & I_k\end{pmatrix}\begin{pmatrix}\phi^{n+1}\\ \mu^{n+1}\\ \bar r^{n+1}\end{pmatrix}=\bar b^n,$$

where I is the identity operator, I_k is the identity matrix of order k, and $\bar b^n$ includes only the terms from previous time steps. We can first solve $\bar r^{n+1}=(r_1^{n+1},\dots,r_k^{n+1})^t$ using a block Gaussian elimination, which requires solving k system with constant coefficients of the form

$$\begin{pmatrix} \frac{1}{\Delta t}I & \mathcal{G}\\ -\mathcal{L} & I\end{pmatrix}\begin{pmatrix}\phi\\ \mu\end{pmatrix}=\bar b.$$

With $\bar r^{n+1}$ known, we can obtain (ϕ^{n+1},μ^{n+1}) by solving one more system in the above form.

Stabilized MSAV approach. In some situations where the nonlinear terms in the free energy are very strong compared with the linear terms, such as in (4.1) with $\epsilon_i \ll 1$, the MSAV approach may need exceedingly small time steps to obtain accurate solutions. In these cases, we may split the free energy in a different manner by adding; suitable stabilized terms to the linear terms. For example, consider (4.1) with $\epsilon_i \ll 1$; we can split it as follows:

$$E(\phi)=\int_\Omega\left[\frac{1}{2}\phi\,\mathcal{L}\phi+\sum_{i=1}^{k}\frac{S_i}{\epsilon_i}\right]+\sum_{i=1}^{k}\frac{1}{\epsilon_i}(F_i(\phi)-S_i)d\boldsymbol{x}, \tag{4.7}$$

where S_i are some suitable positive terms such that $\tilde E_i(\phi):=\int_\Omega\sum_{i=1}^{k}\frac{1}{\epsilon_i}(F_i(\phi)-S_i)d\boldsymbol{x}$ is still bounded from below (this can be easily established, for instance, with typical double-well potentials). We can then apply the MSAV approach with the above splitting of the free energy.

5. Numerical simulations. We now present several numerical experiments to verify the stability and accuracy of the proposed numerical schemes. We set $\Omega=(-\pi,\pi)^d$ $(d=2,3)$ and use the Fourier-spectral method to discretize the space variables. In all computations, we use 129^d Fourier modes with the following parameters:

$$\epsilon=\frac{6\pi}{128},\ M=1. \tag{5.1}$$

5.1. Accuracy tests. We first perform the same simulation presented in Figure 1 using MSAV-BDF2 with the same parameters and plot the results later in Figure 3. We observe that for the two sets of $\eta = \gamma = 0.1, 0.001$, the modified and original energies by the MSAV approach are indistinguishable even at a much larger time step $\Delta t = 0.2 \times 10^{-3}$. This example indicates that for gradient flows with disparate nonlinear terms, such as the constraints enforced by penalty in the free energy, it is essential to use the MSAV approach.

5.1.1. With a manufactured exact solution. We now test the order of convergence with a manufactured exact solution,

$$\phi(x, y, t) = \left(\frac{\sin(2x)\sin(2y)}{4} + 0.48\right)\left(1 - \frac{\sin^2(t)}{2}\right). \tag{5.2}$$

In Table 1, we list the L^2 errors of the phase variable ϕ with volume and surface area constraints ($\eta = \gamma = 0.02$) between the numerical solution and the exact solution at $t = 0.5$ with different time step sizes. We observe that both Scheme 1 and Scheme 2 achieve second-order accuracy in time.

5.1.2. Adaptive time stepping with a given initial condition. We examine here the temporal accuracy of the adaptive time stepping using an example with the initial condition

$$\begin{aligned}\phi(x, y, z, 0) = &\tanh\left(\frac{0.25\pi - \sqrt{x^2 + (y - 0.35\pi)^2 + z^2}}{\sqrt{2}\epsilon}\right) \\ &+ \tanh\left(\frac{0.25\pi - \sqrt{x^2 + (y + 0.35\pi)^2 + z^2}}{\sqrt{2}\epsilon}\right) + 1.\end{aligned} \tag{5.3}$$

We computed the solution without volume and surface area constraints ($M_1 = 0, M_2 = 0$) by using Scheme 3 with adaptive time stepping and Scheme 2 with a very small time step $\delta t = 0.00001$. Evolutions of the scaled energy are shown in Figure 2. We observe that the two results are indistinguishable. Note that for this example, the total number of adaptive steps is 687, while it takes 50000 uniform time steps with $\delta t = 0.00001$, indicating that our adaptive time stepping is very effective.

TABLE 1

Accuracy test: with given exact solution for the PF-VMEM model (2.4)–(2.5). The L^2 errors at $t = 0.5$ for the phase variable ϕ with volume and surface area constraints ($\eta = \gamma = 0.02$), computed by Scheme 1 and Scheme 2 using various time steps.

δt	Scheme 1	Order	Scheme 2	Order
2×10^{-3}	$1.73E(-6)$	–	$3.81E(-6)$	–
1×10^{-3}	$5.15E(-7)$	1.74	$1.32E(-6)$	1.53
5×10^{-4}	$1.32E(-7)$	1.96	$3.90E(-7)$	1.76
2.5×10^{-4}	$3.52E(-8)$	1.91	$1.12E(-7)$	1.80
1.25×10^{-4}	$8.44E(-9)$	2.01	$2.78E(-8)$	2.01
6.25×10^{-5}	$2.06E(-9)$	2.03	$6.91E(-9)$	2.00
3.125×10^{-5}	$5.09E(-10)$	2.02	$1.72E(-9)$	2.00
1.5625×10^{-5}	$1.26E(-10)$	2.01	$4.30E(-10)$	2.00

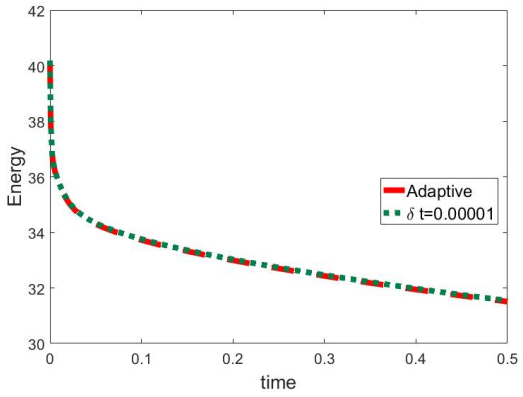

FIG. 2. *Evolution of the free energy using Scheme* 2 *with the time step* $\delta t = 0.00001$ *and Scheme* 3 *with adaptive time stepping.*

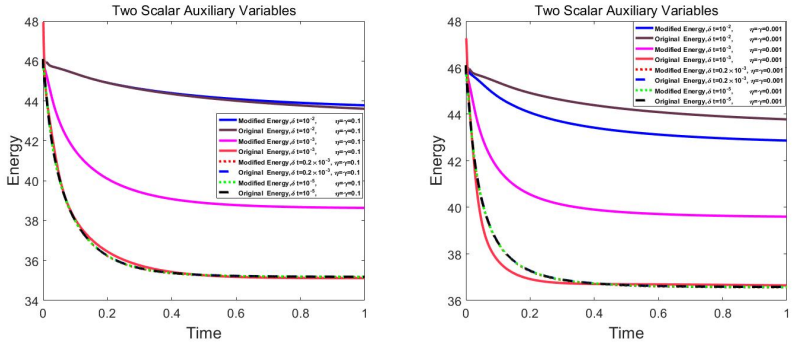

FIG. 3. *Evolution of the modified and original energies by the MSAV Scheme* 2*: Left,* $\eta = \gamma = 0.1$. *Right:* $\eta = \gamma = 0.001$.

In Figure 3, we investigate the accuracy of our schemes with different time steps. We observe that with both $\eta = \gamma = 0.1$ and $\eta = \gamma = 0.0001$, we can obtain accurate results with $\Delta t \sim 10^{-3}$, but the results with $\Delta t \sim 10^{-2}$ deviate significantly while still decaying monotonically. It is interesting to note that with $\Delta t = 10^{-3}$ the modified energy is not accurate but the original energy is essentially correct.

5.1.3. Comparison with ETDRK schemes. Below we make a comparison between our MSAV schemes, with or without adaptive time stepping, with stabilized ETDRK2 and ETDRK4 schemes developed in [20], the initial condition is taken as two close-by spheres in two dimensions which is defined by (5.4), and for the adaptive time stepping method we choose parameter $tol = 10^{-5}$, $\rho = 0.6$, $\delta t_{min} = 10^{-4}$, $\delta t_{max} = 10^{-2}$. From Figure 4, the original energy of the MSAV-BDF2 scheme and adaptive numerical scheme are essentially the same as the energy by ETDRK2. This indicates that the accuracy of our schemes is comparable to that of the ETDRK schemes. Note that we used the stabilized MSAV approach with similar stabilization terms as in the stabilized ETDRK2 scheme.

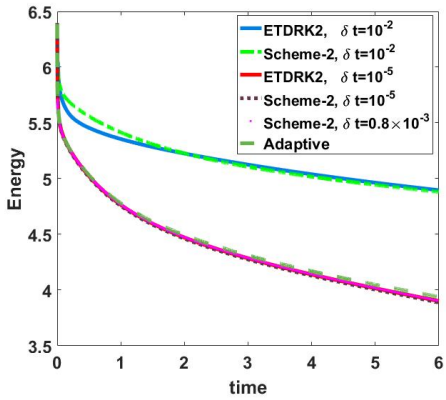

FIG. 4. *Evolution of the original energies by ETDRK2, MSAV-BDF2 (Scheme 2), and the adaptive scheme (Scheme 3).*

$$\phi(x,y,0) = \tanh\left(\frac{0.28\pi - \sqrt{x^2+(y-0.35\pi)^2}}{\sqrt{2}\epsilon}\right) + \tanh\left(\frac{0.28\pi - \sqrt{x^2+(y+0.35\pi)^2}}{\sqrt{2}\epsilon}\right) + 1. \tag{5.4}$$

5.2. Collision of two close-by spherical vesicles for the PF-VMEM model. We use the following initial condition for ϕ to describe two close-by spherical vesicles in three dimensions:

$$\phi(x,y,z,0) = \tanh\left(\frac{0.28\pi - \sqrt{x^2+y^2+(z-0.35\pi)^2}}{\sqrt{2}\epsilon}\right) + \tanh\left(\frac{0.28\pi - \sqrt{x^2+y^2+(z+0.35\pi)^2}}{\sqrt{2}\epsilon}\right) + 1, \tag{5.5}$$

and we use Scheme 2 with time step $\delta t = 0.0001$ to study the collision of the two close-by spherical vesicles.

In Figure 5, we depict the collision process without the volume and surface constraints. We observe that the two close-by spheres will gradually merge into one capsule shape and eventually become a ball which is the steady state solution.

We then impose the volume and surface constraints with the penalty parameters $\alpha = \eta = 0.02$ and $\alpha = \eta = 0.0001$ and plot the results in Figures 6 and 7, respectively. The two sets of results are visually indistinguishable. We observe that the two spheres connect within a small time interval, then merge into a stable capsule shape.

In Figure 8, we plot the evolution of original energy, the difference of volume and surface area, with and without the volume and surface area constraints. We observe that in both cases the original energy decays rapidly, and the volume and surface area are well preserved under the volume and surface area constraints where the constraint parameters $\eta = \gamma = 0.001$.

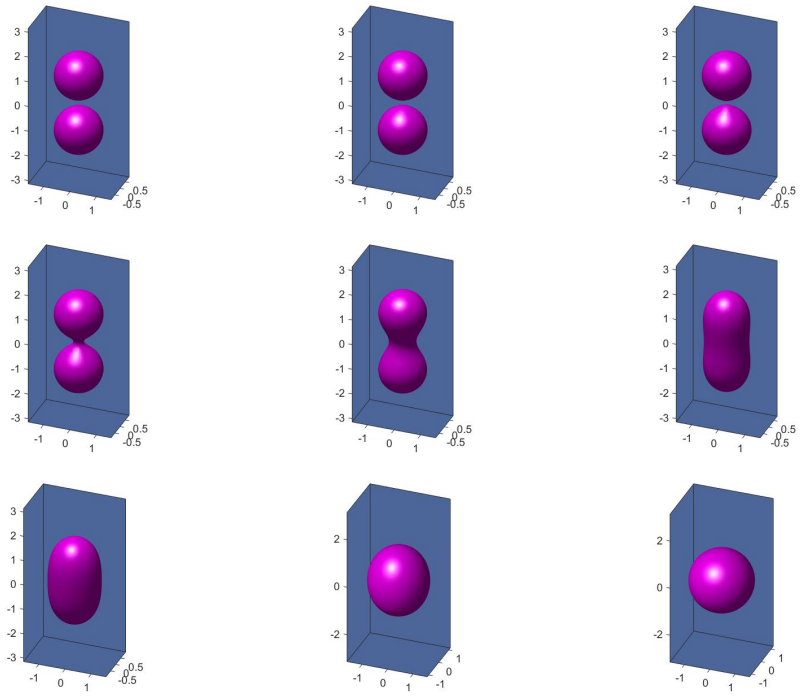

FIG. 5. *Collision of two close-by spherical vesicles without the volume and surface area constraints using Scheme* 2 *with the time step size* $\delta t = 0.0001$. *Snapshots of the iso-surfaces of* $\phi = 0$ *at* $t = 0, 0.005, 0.01, 0.02, 0.1, 0.5, 1, 2, 6$.

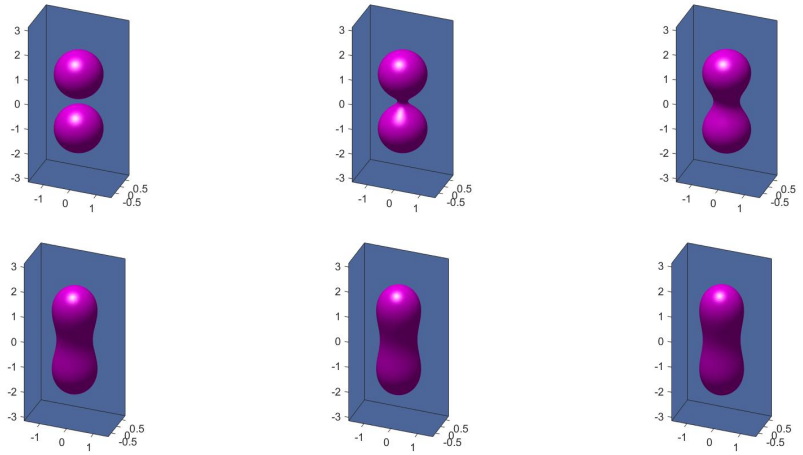

FIG. 6. *Collision of two three-dimensional close-by spherical vesicles with the volume and surface area constraints* ($\eta = \gamma = 0.02$) *using Scheme* 2 *with the time step size* $\delta t = 0.0001$. *Snapshots of the iso-surfaces of* $\phi = 0$ *at* $t = 0, 0.02, 0.1, 0.5, 1, 2$.

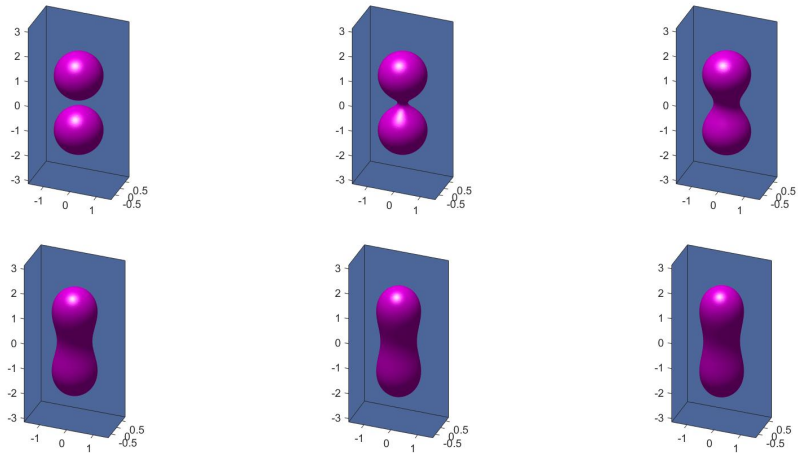

FIG. 7. *Collision of two three-dimensional close-by spherical vesicles with the volume and surface area constraints ($\eta = \gamma = 0.001$) using Scheme 2 with the time step size $\delta t = 0.0001$. Snapshots of the iso-surfaces of $\phi = 0$ at $t = 0, 0.02, 0.1, 0.5, 1, 2$.*

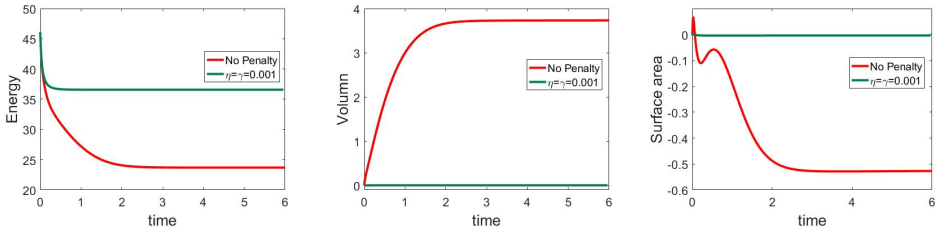

FIG. 8. *Evolution of the original energy, the volume difference $A(\phi) - \alpha$, and the surface area difference $B(\phi) - \beta$ with and without the volume and surface area constraints using Scheme 2 with the time step size $\delta t = 0.0001$.*

5.3. Deformation of an ellipsoid. We simulate here the deformation of an ellipsoid vesicle in the PF-VMEM model with the initial profile

$$\phi(x, y, z, 0) = \tanh\left(\frac{1 - \sqrt{x^2/4 + y^2 + z^2}}{\sqrt{2}\epsilon}\right). \tag{5.6}$$

We use Scheme 2 with time step $\delta t = 0.0001$ and plot the results without volume and surface area constraints in Figure 9. We observe that the ellipsoid gradually evolves into a spherical shape at time $t = 6$.

In Figure 10, we plot the results with volume and surface area constraint parameter $\eta = \gamma = 0.001$. We observe the ellipsoid gradually evolves into the stable shape at time $t = 6$, which is different from Figure 9.

5.4. Collision of four close-by spherical vesicles. As the last example, we simulate the collision process of four close-by spherical vesicles which are initially given as

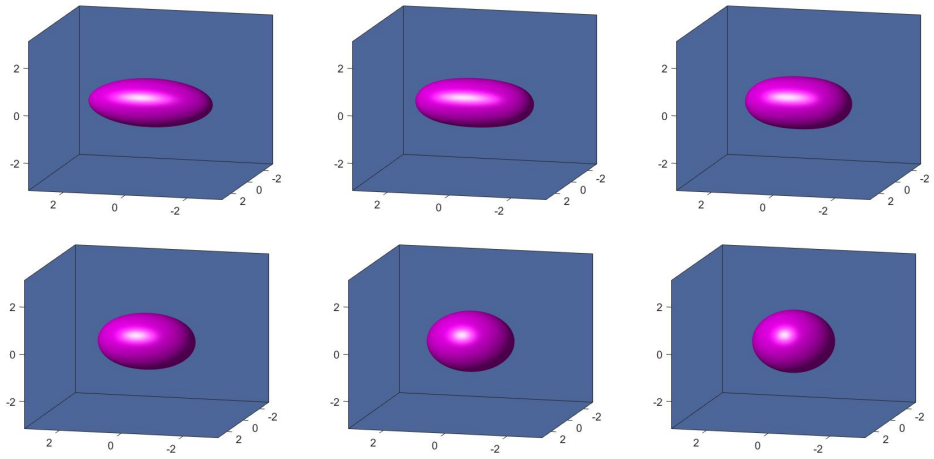

FIG. 9. *The dynamical behaviors of the ellipsoid vesicles without the volume and surface area constraints using Scheme* 2 *with the time step size* $\delta t = 0.0001$. *Snapshots of the numerical approximation of the iso-surfaces of* $\phi = 0$ *are taken at* $t = 0, 0.1, 0.5, 1, 2, 6$.

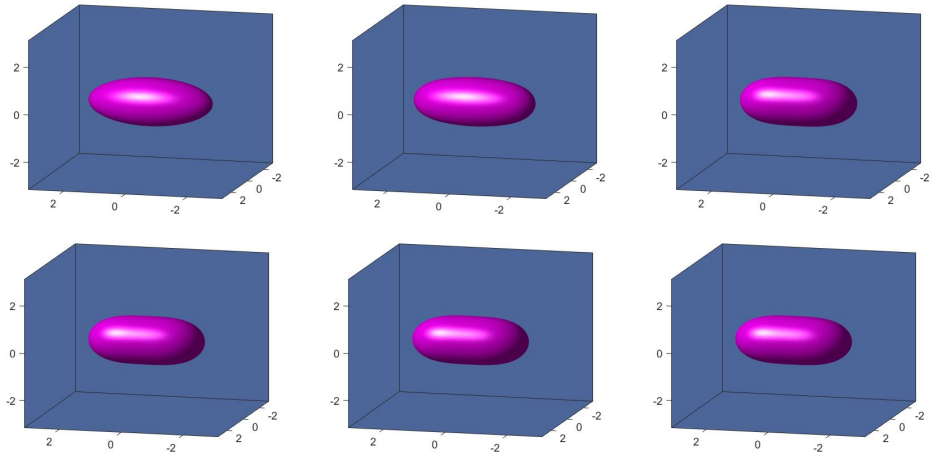

FIG. 10. *The dynamical behaviors of the ellipsoid vesicles with the volume and surface area constraints (i.e.,* $\eta = \gamma = 0.001$*) using Scheme* 2 *with the time step size* $\delta t = 0.0001$. *Snapshots of the numerical approximation of the iso-surfaces of* $\phi = 0$ *are taken at* $t = 0, 0.1, 0.5, 1, 2, 6$.

$$
\begin{aligned}
\phi(x,y,z,0) = \tanh&\left(\frac{\frac{\pi}{6} - \sqrt{(x+\frac{\pi}{4})^2 + (y+\frac{\pi}{4})^2 + z^2}}{\sqrt{2}\epsilon}\right) \\
&+ \tanh\left(\frac{\frac{\pi}{6} - \sqrt{(x+\frac{\pi}{4})^2 + (y-\frac{\pi}{4})^2 + z^2}}{\sqrt{2}\epsilon}\right) \\
&+ \tanh\left(\frac{\frac{\pi}{6} - \sqrt{x^2 + (y-\frac{\pi}{4})^2 + z^2}}{\sqrt{2}\epsilon}\right) \\
&+ \tanh\left(\frac{\frac{\pi}{6} - \sqrt{x^2 + y^2 + (z-\frac{\pi}{3})^2}}{\sqrt{2}\epsilon}\right) + 3.
\end{aligned} \tag{5.7}
$$

We use Scheme 2 with time step $\delta t = 0.0001$ and plot the results without volume and surface area constraints in Figure 11 and those with volume and surface area constraints in Figure 12. We observe from Figure 11 that the initially four disjoint spheres merge and eventually evolve into a ball, which is similar to the collision of two spheres in Figure 5. However, when we add the volume and surface area constraints with $\eta = \gamma = 0.001$, the four spheres will merge and eventually evolve into a doughnut shape.

Next we examine the influence of the penalty parameters. In Figure 13, we plot the results with smaller volume and surface area constraint parameters $\eta = \gamma = 0.02$. We observe that the evolution process up to time $t = 0.5$ is essentially the same as in Figure 12 with $\eta = \gamma = 0.001$. However, it eventually evolves into a capsule shape, which is very different from the ball shape at $t = 2$ in Figure 12.

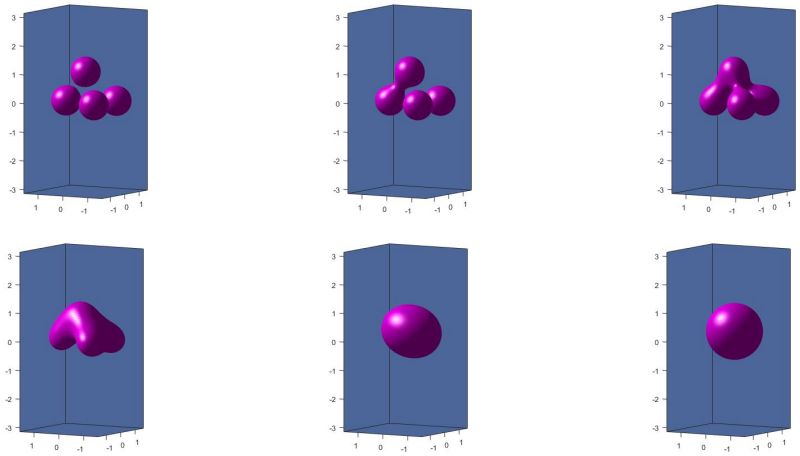

FIG. 11. *The dynamical behaviors of four spherical vesicles without the volume and surface area constraints using Scheme* 2 *with the time step size* $\delta t = 0.0001$. *Snapshots of the numerical approximation of the iso-surfaces of* $\phi = 0$ *are taken at* $t = 0, 0.005, 0.002, 0.1, 0.5, 2$.

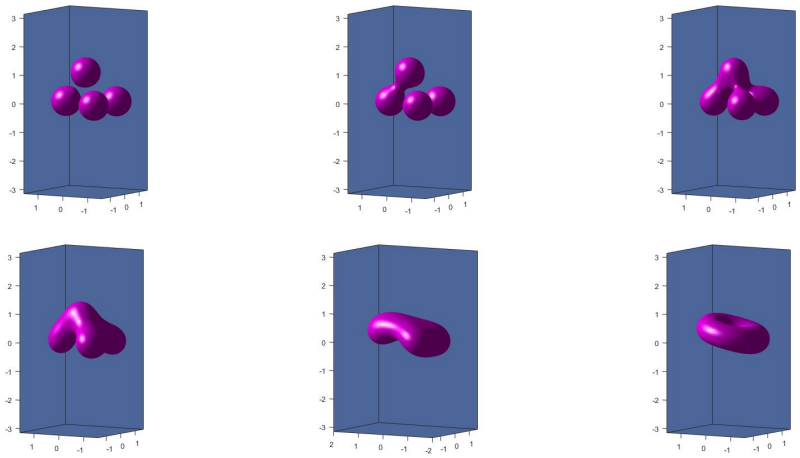

FIG. 12. *Collision of four spherical vesicles with the volume and surface area constraints (i.e.,* $\eta = \gamma = 0.001$*). Snapshots of the iso-surfaces of* $\phi = 0$ *at* $t = 0, 0.005, 0.002, 0.1, 0.5, 2$.

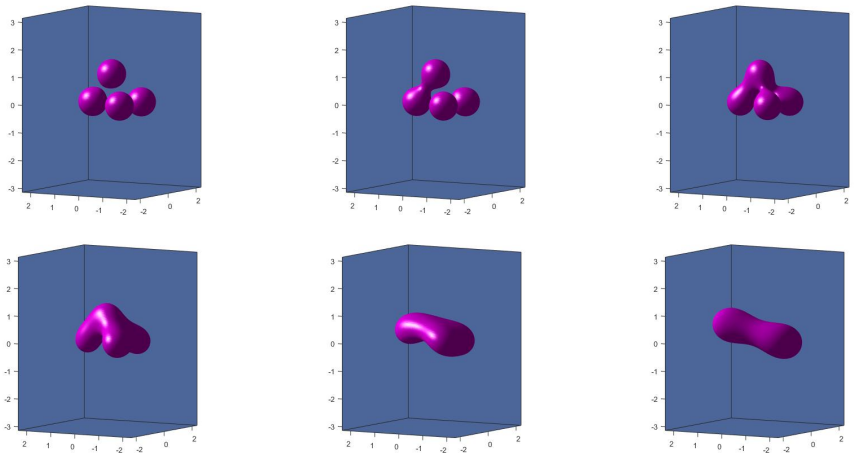

FIG. 13. *Collision of four spherical vesicles with the volume and surface area constraints (i.e.,* $\eta = \gamma = 0.02$*). Snapshots of the iso-surfaces of* $\phi = 0$ *at* $t = 0, 0.005, 0.002, 0.1, 0.5, 2$.

6. Concluding remarks. We developed in this paper the MSAV approach for gradient flows with disparate terms in the free energy that cannot be efficiently handled with the SAV approach and applied it to the PF-VMEM model, which, in addition to some usual nonlinear terms in the free energy, has two additional penalty terms to enforce the volume and surface area. Our numerical results indicated that while the SAV approach could be applied to the PF-VMEM model, it was not able to produce correct numerical solutions even with very small time steps. The main reason is that the two additional penalty terms behave very differently with the other nonlinear terms and cannot be properly handled with a single auxiliary variable. Noticing that the volume penalty term leads to a linear term in the PDE system so it can be treated implicitly along with other linear terms, we introduced one additional SAV for the surface area constraint and developed the so-called MSAV approach, which enjoys the same computational advantages as the SAV approach but can handle free energies with multiple disparate terms such as multiple constraints enforced through penalty in the free energy. More precisely, the MSAV schemes enjoy the following advantages:

- are second-order accurate in time;
- are unconditionally energy stable; and
- lead to decoupled elliptic equations with constant coefficients to solve at each time step.

Thus, these schemes are easy to implement and extremely efficient, usually only taking a fraction of the computing time required by existing methods. We also constructed a second-order MSAV scheme with variable time steps so that it can be used with an adaptive time stepping.

We presented ample numerical results to validate the stability and accuracy of these schemes. It is clear that the MSAV approach presented here can be used to deal with other gradient flows with constraints.

We have only established energy stability for our MSAV schemes in this paper. However, a rigorous convergence and error analysis for the SAV approach under a general setting has been established in [17]. It is expected that similar convergence

and error estimates would hold for the MSAV schemes, and detailed analysis will be carried out elsewhere.

Although we considered only semidiscretized schemes in time in this paper, the stability results here can be carried over to any consistent finite-dimensional Galerkin type approximations since the proofs are all based on a variational formulation with all test functions in the same space as the trial functions.

REFERENCES

[1] P. B. Canham, *The minimum energy of bending as a possible explanation of the biconcave shape of the human red blood cell*, J. Theoret. Biol., 26 (1970), pp. 61–81.

[2] R. S. Chadwick, *Axisymmetric indentation of a thin incompressible elastic layer*, SIAM J. Appl. Math., 62 (2002), pp. 1520–1530.

[3] R. Chen, G. Ji, X. Yang, and H. Zhang, *Decoupled energy stable schemes for phase-field vesicle membrane model*, J. Comput. Phys., 302 (2015), pp. 509–523.

[4] Q. Du, M. Li, and C. Liu, *Analysis of a phase field navier-stokes vesicle-fluid interaction model*, Discrete Contin. Dyn. Syst. Ser. B, 8 (2007), pp. 539–556.

[5] Q. Du, C. Liu, and X. Wang, *A phase field approach in the numerical study of the elastic bending energy for vesicle membranes*, J. Comput. Phys., 198 (2004), pp. 450–468.

[6] Q. Du, C. Liu, and X. Wang, *Simulating the deformation of vesicle membranes under elastic bending energy in three dimensions*, J. Comput. Phys., 212 (2006), pp. 757–777.

[7] C. M. Elliott and A. M. Stuart, *The global dynamics of discrete semilinear parabolic equations*, SIAM J. Numer. Anal., 30 (1993), pp. 1622–1663.

[8] D. J. Eyre, *Unconditionally gradient stable time marching the Cahn-Hilliard equation*, in Computational and Mathematical Models of Microstructural Evolution (San Francisco, CA, 1998), Mater. Res. Soc. Sympos. Proc. 529, MRS, Warrendale, PA, 1998, pp. 39–46.

[9] H. Gomez and T. J. Hughes, *Provably unconditionally stable, second-order time-accurate, mixed variational methods for phase-field models*, J. Comput. Phys., 230 (2011), pp. 5310–5327.

[10] R. Gu, X. Wang, and M. Gunzburger, *A two phase field model for tracking vesicle–vesicle adhesion*, J. Math. Biol., 73 (2016), pp. 1293–1319.

[11] F. Guillén-González and G. Tierra, *Unconditionally energy stable numerical schemes for phase-field vesicle membrane model*, J. Comput. Phys., 354 (2018), pp. 67–85.

[12] W. Helfrich, *Elastic properties of lipid bilayers: theory and possible experiments*, Z. Naturforschung C, 28 (1973), pp. 693–703.

[13] J. S. Lowengrub, A. Rätz, and A. Voigt, *Phase-field modeling of the dynamics of multicomponent vesicles: Spinodal decomposition, coarsening, budding, and fission*, Phys. Rev. E, 79 (2009), 031926.

[14] Z. Qiao, Z. Zhang, and T. Tang, *An adaptive time-stepping strategy for the molecular beam epitaxy models*, SIAM J. Sci. Comput., 33 (2011), pp. 1395–1414.

[15] J. Shen, T. Tang, and J. Yang, *On the maximum principle preserving schemes for the generalized Allen–Cahn equation*, Commun. Math. Sci, 14 (2016), pp. 1517–1534.

[16] J. Shen, C. Wang, X. Wang, and S. M. Wise, *Second-order convex splitting schemes for gradient flows with Ehrlich-Schwoebel type energy: application to thin film epitaxy*, SIAM J. Numer. Anal., 50 (2012), pp. 105–125.

[17] J. Shen and J. Xu, *Convergence and error analysis for the scalar auxiliary variable (SAV) schemes to gradient flows*, SIAM J. Numer. Anal., 56 (2018), pp. 2895–2912.

[18] J. Shen, J. Xu, and J. Yang, *The scalar auxiliary variable (sav) approach for gradient flows*, J. Comput. Phys., 353 (2018), pp. 407–416.

[19] X. Wang and Q. Du, *Modelling and simulations of multi-component lipid membranes and open membranes via diffuse interface approaches*, J. Math. Biol., 56 (2008), pp. 347–371.

[20] X. Wang, L. Ju, and Q. Du, *Efficient and stable exponential time differencing Runge–Kutta methods for phase field elastic bending energy models*, J. Comput. Phys., 316 (2016), pp. 21–38.

[21] X. Yang, *Linear, first and second-order, unconditionally energy stable numerical schemes for the phase field model of homopolymer blends*, J. Comput. Phys., 327 (2016), pp. 294–316, https://doi-org.ezproxy.lib.purdue.edu/10.1016/j.jcp.2016.09.029.

[22] X. Yang and L. Ju, *Efficient linear schemes with unconditional energy stability for the phase field elastic bending energy model*, Comput. Methods Appl. Mech. Engrg., 315 (2017), pp. 691–712.

[23] P. Yue, J. J. Feng, C. Liu, and J. Shen, *A diffuse-interface method for simulating two-phase flows of complex fluids*, J. Fluid Mech., 515 (2004), pp. 293–317.
[24] C. W. Z. Hu, S. M. Wise, and J. S. Lowengrub., *Stable and efficient finite difference nonlinear-multigrid schemes for the phase field crystal equation*, J. Comput. Phys, 228 (2009), pp. 5323–5339.
[25] J. Zhang, S. Das, and Q. Du, *A phase field model for vesicle–substrate adhesion*, J. Comput. Phys., 228 (2009), pp. 7837–7849.